

Exploring the effects of tuned mass dampers on the seismic performance of structures with nonlinear base isolation systems

Reza Mirza Hessabi^{*1}, Oya Mercan^{1a} and Baki Ozturk^{2a}

¹Department of Civil Engineering, University of Toronto, 35 St. George Street, Toronto, ON, M5S 1A4, Canada

²Civil Engineering Department, Hacettepe University, Ankara, Turkey

(Received May 4, 2016, Revised February 6, 2017, Accepted February 12, 2017)

Abstract. Base isolation is a quite practical control strategy for enhancing the response of structural systems induced by strong ground motions. Due to the dynamic effects of base isolation systems, reduction in the interstory drifts of the superstructure is often achieved at the expense of high base displacement level, which may lead to instability of the structure or non-practical designs for the base isolators. To reduce the base displacement, several hybrid structural control strategies have been studied over the past decades. This study investigates a particular strategy that employs Tuned Mass Dampers (TMDs) for improving the performance of base-isolated structures and unlike previous studies, specifically focuses on the effectiveness of this hybrid control strategy in structures that are equipped with nonlinear base isolation systems. To consider the nonlinearities of base isolation systems, a Bouc-Wen model is selected and nonlinear dynamic OpenSees models are used to perform several time-history simulations in time and frequency domains. Through these numerical simulations, the effects of several parameters such as the fundamental period of the structure, dynamic properties of the TMD and isolation systems and properties of the input ground motion on the behaviour of TMD-structure-base isolation systems are examined. The results of this study provide a better insight into the performance of linear shear-story structures with nonlinear base isolators and show that there are many scenarios in which TMDs can still improve the performance of these systems.

Keywords: structural control; tuned mass damper; base isolation; nonlinear dynamic analysis; earthquake engineering

1. Introduction

Due to major developments in the theory and application of base isolation and supplemental energy dissipation devices in recent years, considerable advances have been accomplished in the area of seismic protection of structures. Seismic isolation involves using isolators, which possess much lower lateral stiffness than the lateral stiffness of the structure and hence elongating the structural period of vibration. From the energy point of view, the seismic isolation system separates the superstructure from the ground motion and limits the seismic energy transfer to the structure (Mahmoud *et al.* 2012). Another successful strategy for controlling the seismic response of structures is the application of dynamic vibration absorbers such as TMDs, which are commonly composed of a mass, a damping device and a spring that are linked to the main structure. Generally, TMDs are designed to oscillate with the same period as the primary system but in an opposite phase. By tuning the natural frequency of these devices to the dominant mode of vibration of the primary structure, a considerable reduction in the dynamic response of the primary structure can be achieved (Chung *et al.* 2009, Matta 2015, Esteki *et al.* 2015).

Yet, despite their numerous implementations in real buildings, both of these systems have some limitations and undesirable side effects. In base-isolated structures, displacement and yielding are concentrated at the level of the isolation devices, and the superstructure behaves very much like a rigid body. In other words, higher performance of these systems is usually obtained at the expense of a considerable increase in the deformability at the isolation level, which may lead to amplification in the structural response under certain ground motions. For instance, in a parametric study of linear seismic isolation systems for buildings, Alhan and Gavin (2004) showed that the base drift always increases with decreased isolation stiffness for all of the earthquake records that were considered in their study. To diminish the excessive base displacement, some passive control devices with energy dissipation capacity have been proposed and applied in practice (Ribakov 2010). Conventional techniques solve this problem by providing supplemental viscous or hysteretic damping (Politopoulos 2008). It is shown by several researchers that although a supplemental viscous damping at the base is appropriate for controlling the isolator displacement, at the same time, it increases the contribution of higher vibration modes of the superstructure and depending on the frequency content of the seismic input, the additional damping may have adverse effects. Increasing damping can lead to a significant amplification of the inter-story drifts and floor accelerations values near the higher mode frequencies (Alhan and Gavin 2004). This means that the additional damping does not always guarantee a better performance for the

*Corresponding author, Ph.D.

E-mail: reza.hessabi@mail.utoronto.ca

^aAssociate Professor

superstructure (Mazza and Vulcano 2009, Kelly 1999). Mainly due to the effects of the discontinuity of the friction force, hysteretic damping is even less efficient than linear viscous damping as it leads to higher accelerations. In particular, approximately around the higher natural frequencies of the system, additional hysteretic damping amplifies the shear forces and floor spectral values (Politopoulos 2008).

Introducing a TMD into a regular fixed-base structure as a passive control strategy can have several disadvantages. Since TMDs are tuned (i.e., their dynamic parameters are optimized) to the fundamental natural period of the structure, these devices are most effective when the input ground motion has a dominant resonance frequency. However, when the systems are excited by ground motions with other dominant frequencies, the effectiveness of stand-alone TMDs reduces. Besides, the earthquake motion may induce significant higher-mode response for which the TMD is not designed for. Moreover, the stiffness property of the structure may change over time due to large displacements and cracking, which can lead to detuning of the TMD.

By combining a TMD with a base isolation system, each of these two systems can compensate for the problems of the other one, and it can lead to a more robust combined control system (Taniguchi 2008). The improved behaviour of the combined system compared to the original structure can be described in terms of three different effects. First, similar to the isolated systems without TMDs, by shifting the structure's fundamental frequency, the energy transmission of the ground motion to the superstructure is reduced. Secondly, the isolator modifies the vibration modes, and the superstructure mainly vibrates as a rigid body. This diminishes the higher mode effects. Finally, the TMD is tuned to this dominant frequency to enhance the response of the structure (Palazzo and Petti 1999). As a result, the base isolator can be used to improve the behaviour of the structure, and the TMD can be used to reduce the undesirable large displacements at the isolation level.

Most of the studies in the literature are concerned with the analysis of TMD effectiveness on systems with linear base isolators. Yang *et al.* (1990), studied the influence of both passive and active mass dampers in reducing the response of tall buildings under strong earthquakes. Their research showed that a sufficient decrease in the displacement of base isolation systems could be obtained by including a passive/active TMD. However, the reduction of peak displacement response of the structures during the first few seconds of earthquake excitations was found to be insufficient to describe the TMD effectiveness. The results indicated that a reduction in the displacement requires a large displacement of the mass damper and for this reason, TMD are not very effective at the beginning of the excitation (Tsai 1995). Other studies also demonstrated that the use of TMDs on base isolated structures reduces the displacement demands, especially for isolation systems with lower damping (Palazzo *et al.* 1997, Xiang and Nishitani 2014). Petti *et al.* (2010) performed a series of experiments on a small-scale three degree of freedom models to verify

the numerical results of previous studies experimentally. Zhang and Phillips (2015), proposed base isolation with linear isolators for the protection of structures under blast loading and employed TMDs to improve the overall RMS behaviour of the base isolated structures. They reported that the base isolated system with a TMD exhibited significant reductions in RMS values for base displacement, interstory drifts, and absolute story accelerations.

Unlike the linear systems, there is little information in the literature about the application of TMD to nonlinear isolators. Alhan and Gavin (2004) showed that for buildings with nonlinear base isolation systems and without TMDs, increasing the yield force and decreasing the yield displacement leads to the reduction of the base drifts. However, inter-story drifts and floor accelerations are not always reduced by changing the yield force and displacement. They also showed that the performance of the nonlinear base isolated structures depends on the type of earthquake record. As a result, there is a need to study the effects of the addition of TMDs to buildings with nonlinear base isolation systems separately.

Perhaps Sinha and Li (1994) are among the first researchers who looked at this problem. In their bilinear hysteretic model, they only considered the 1971 San Fernando earthquake data and evaluated the maximum angular displacement of the isolator. Their results revealed that for reasonably low TMD mass ratios, the response could be improved significantly. In another study, Palazzo and Petti (1999) confirmed this result by concluding that the use of TMD could always result in the reduction of isolator displacements even in the presence of nonlinear isolation systems. In another study, same authors carried out a new study to investigate the effectiveness of this strategy in reducing the seismic displacement demand of nonlinear isolated structures (2008). They observed that although this control strategy is less effective than in the case of linear isolators, it is still capable of reducing the peak isolator displacements by 10 percent. However, their study is model-specific and can be limited to the results obtained for the benchmark structure.

Considering the limitations of each of the previous studies, in the present study, the efficiency of the strategy to adopt TMDs to improve the nonlinear seismic response of structures is investigated and compared to the results from uncontrolled base isolated structures and with those from structures with linear isolators. An extensive parametric study is carried out to examine the importance of dynamic parameters better.

2. Dynamic analysis of the system

2.1 Equations of motion

A schematic presentation of the system which is considered in this study is shown in Fig. 1. This base isolated structure-TMD systems (BITMD) consists of an N story steel shear building (i.e., primary structure or superstructure) on top of a base isolator. Depending on the analysis, the base isolation system can be chosen to be

either linear or nonlinear. To investigate the effectiveness of TMDs, the base isolated structure is equipped with a linear mass damper attached to the highest degree of freedom of the superstructure. The variables x_b and x_t are the base isolation and TMD displacements, respectively; whereas \ddot{x}_g denotes the support acceleration applied to the system. Similarly, x_i refers to the displacements of the i th degree of freedom of the superstructure. m , c , and k show the mass, damping coefficient and stiffness of the system components, respectively and will be changed in this part of this study to analyze and examine the seismic performance of the BITMD system.

To describe the behaviour of base isolation systems, several mathematical models have been proposed in the literature. These systems can be modeled with both linear and nonlinear elements. For the most straightforward case, Hooke's law can be used to describe the behaviour of a conventional linear isolator such as laminated-rubber bearings (elastomeric bearings). Although these models have been used extensively in the past, the application of these systems in the real world is limited. For this reason, this study emphasizes on base isolation systems with nonlinear behaviour. Two main types of these systems that have been widely used over the past two decades are lead-rubber bearings and friction pendulum systems. The friction pendulum system consists of an articulated friction slider that travels on a spherical concave lining surface. The typical hysteretic behaviour of these systems, which can be

modeled with piecewise linear models, is shown in Fig. 2(a). In addition to bilinear models, the Bouc-Wen model can be used to model more complex force-displacement hysteretic loops such as the ones that are exhibited by lead-rubber bearings (Palazzo and Petti 1999, Sinha and Li 1994). Bouc-Wen (BW) model (Wen 1976) was introduced by Bouc and extended by Wen, who demonstrated its versatility by producing a variety of hysteretic characteristics. The BW model can match a hysteretic behaviour by properly tuning its parameters (Fig. 2(b)).

In the present study, the behaviours of the isolators are described by linear and BW models with appropriately chosen parameters. The general equations of motion for this system can be described with the following $N+2$ equations, as shown in Eqs. (1)-(5) (Mirza Hessabi *et al.* 2014)

$$m_b \ddot{x}_b + R_b(x_b, \dot{x}_b) - R_1(x_b, x_1, \dot{x}_b, \dot{x}_1) = -m_b \ddot{x}_g(t) \quad (1)$$

$$m_1 \ddot{x}_1 + R_1(x_b, x_1, \dot{x}_b, \dot{x}_1) - R_2(x_1, x_2, \dot{x}_1, \dot{x}_2) = -m_1 \ddot{x}_g(t) \quad (2)$$

$$m_i \ddot{x}_i + R_i(x_{i-1}, x_i, \dot{x}_{i-1}, \dot{x}_i) - R_{i+1}(x_i, x_{i+1}, \dot{x}_i, \dot{x}_{i+1}) = -m_i \ddot{x}_g(t) \quad (3)$$

$$m_N \ddot{x}_N + R_N(x_{N-1}, x_N, \dot{x}_{N-1}, \dot{x}_N) - R_t(x_N, x_t, \dot{x}_N, \dot{x}_t) = -m_N \ddot{x}_g(t) \quad (4)$$

$$m_t \ddot{x}_t + R_t(x_N, x_t, \dot{x}_N, \dot{x}_t) = -m_t \ddot{x}_g(t) \quad (5)$$

where, x , \dot{x} and \ddot{x} characterize the displacement, velocity and acceleration of each degree of freedom (DOF) and subscripts b and t denote the base isolation and TMD properties, respectively. The values of R for each DOF can be defined based on the linear/nonlinear model considered. For linear base isolation systems, $R_b(x_b, \dot{x}_b)$ can be obtained from Eq. (6)

$$R_b(x_b, \dot{x}_b) = c_b \dot{x}_b + k_b x_b \quad (6)$$

and Eq. (7) can be used for all of the other degrees of freedom ($j=1, 2, \dots, N-1, N, t$)

$$R_j(x_{j-1}, x_j, \dot{x}_{j-1}, \dot{x}_j) = c_j (\dot{x}_j - \dot{x}_{j-1}) + k_j (x_j - x_{j-1}) \quad (7)$$

These equations can be modified to describe the force displacement relationship of a base isolation system with a BW model (as shown in Fig. 2(b)). Shown in the figure are the characteristic force, Q_y , the yield displacement, D_y , the pre-yield stiffness, k_e and the post-yield stiffness, k_y . Post-yield to pre-yield stiffness ratio ($\alpha = k_y/k_e$) depends on the material used and typically attains values around 0.05 to 0.15. For the nonlinear BW model, $R_b(x_b, \dot{x}_b)$ is calculated from Eqs. (8)-(9) (Ikhouane *et al.* 2007)

$$R_b(x_b, \dot{x}_b) = c_b \dot{x}_b + k_{yb} x_b + \left(1 - \frac{k_{yb}}{k_{eb}}\right) Q_y z_b \quad (8)$$

where, the auxiliary variable z_b should satisfy Eq. (9)

$$\dot{z}_b = -\gamma |\dot{x}_b| |z_b|^{(n-1)} z_b - \beta \dot{x}_b |z_b|^n + A \dot{x}_b \quad (9)$$

In Eqs. (8)-(9), β , γ and A are parameters that control the hysteretic loop shape and n affects the smoothness of the hysteretic curve. In this study, n is assumed to be equal

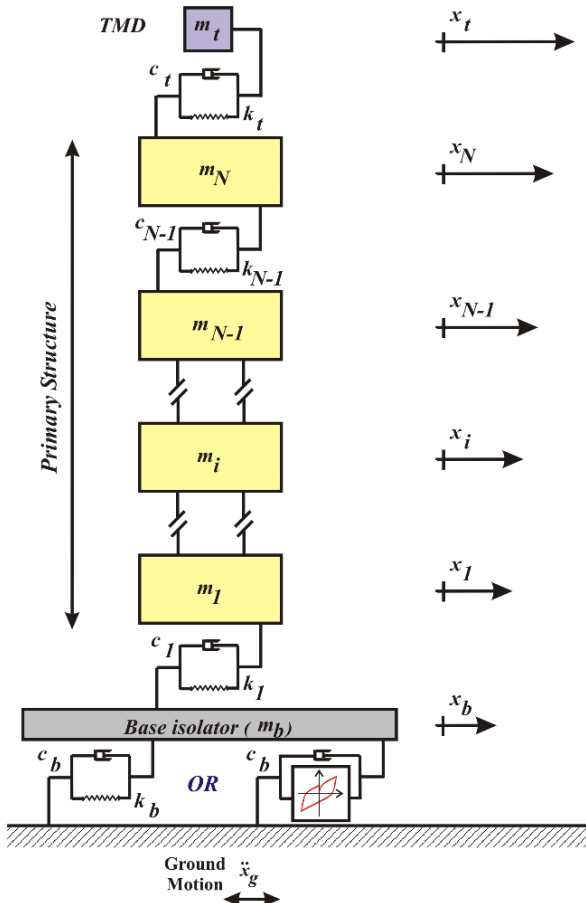


Fig. 1 Idealized model of a BITMD system

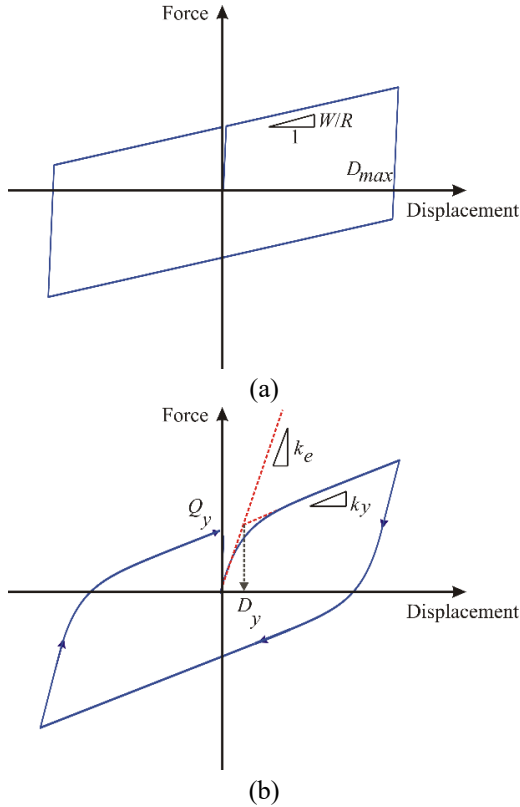


Fig. 2 (a) Piecewise linear, and (b) Bouc-Wen constitutive laws

to unity, and β and γ can be computed using Eq. (10). It was found that these values could properly describe the bilinear backbone of the BW models

$$\beta = \gamma = 0.5 \left(\frac{k_e}{Q_y} \right) \quad (10)$$

2.2 Tuning of the tuned mass damper

A close look at the available literature on the application of TMDs in earthquake engineering shows that there are several equations and methods for designing a TMD for any given structure. In most of these design formulas, the structure is treated as a single-degree-of-freedom (SDOF) oscillator, and the frequency of the damper is chosen to coincide with the principle vibrational frequency of the primary structure. However, civil engineering structures can rarely be considered as single-degree-of-freedom systems and may experience nonlinear behaviour. In addition, earthquake excitations are random in nature. Thus, various optimization criteria have been taken into consideration for this purpose. In this study, the design equations proposed by Tsai (1995) are considered. These equations are shown in Eqs. (11)-(12), respectively. Alternatively, simpler design equations such as those proposed by Den Hartog (1985) can be used. To derive Eqs. (11)-(12), a numerical searching procedure is used to find the optimum parameters for linear damped systems when they are subjected to the two different harmonic excitation sources, fixed-displacement

support motion and fixed-acceleration support motion. These two explicit formulae for the optimum tuning frequency and damping ratio of the TMD were obtained by a sequence of curve-fitting schemes (Tsai and Lin 1993)

$$k_t = k_{eq} \varepsilon \left\{ \begin{array}{l} \left(\frac{\sqrt{1-0.5\varepsilon}}{1+\varepsilon} + \sqrt{1-2\zeta_p^2} - 1 \right) \\ - (2.38 - 1.03\sqrt{\varepsilon} - 0.43\varepsilon)\sqrt{\varepsilon}\zeta_p \\ - (3.73 - 16.90\sqrt{\varepsilon} - 20.5\varepsilon)\sqrt{\varepsilon}\zeta_p^2 \end{array} \right\}^2 \quad (11)$$

$$\zeta_t = \sqrt{\frac{3\varepsilon}{8(1+\varepsilon)(1-0.5\varepsilon)} + (0.15\zeta_p - 0.17\zeta_p^2) + (0.16\zeta_p + 4.98\zeta_p^2)\varepsilon} \quad (12)$$

where, k_t and ζ_t are stiffness and damping ratio of the TMD and ζ_p is the damping ratios of the structure. Also, ε is the mass ratio of the TMD defined as $m_t / \left(m_b + \sum_{i=1}^{N-2} m_i \right)$.

To demonstrate the effects of the TMD more clearly, except for the parametric study of Section 3.3, a value of 10 percent is selected for ε in this study.

Another important parameter in Eqs. (11)-(12) is k_{eq} which is the equivalent stiffness of the base isolator and should be defined for each model separately. Several simplified methods, such as equivalent linearization method and the method using inelastic response spectra, have been proposed for evaluating the inelastic response of structures to the earthquake ground motion. However, in the current application, due to the properties of the base isolation systems, the primary structure usually remains elastic. Thus, the main objective is to find a simplified representation of the structure with the nonlinear base isolation that can be used to design the TMD. To investigate the effects of the nonlinearity of the BITMD system, five different models are considered to define k_{eq} in Eq. (11) and design the TMD.

Model I with a linear base isolator is considered as the control model. In other words, for *Model I*, not only k_{eq} is equal to the pre-yield stiffness, k_e , but also the model in the simulation is linear. In all other models BW model shown in Fig. 2 is used to describe the behaviour of the base isolation elements. In *Model II* and *Model III*, the upper and lower bounds for the equivalent stiffness are used to design the TMD. The value of k_{eq} in these two particular models is assumed to be equal to k_e and k_y . The “geometrical equivalent linearization method” is used to estimate k_{eq} in *Model IV* (Jennings 1968). In this approach, the equivalent stiffness of the equivalent bilinear model of the BW model in Fig. 2 can be expressed as

$$k_{eq} = \frac{1 + \alpha(\mu - 1)}{\mu} k_e \quad (13)$$

where, $\mu = D_{max}/D_y$.

Finally, using the “harmonic balance method,” the equivalent stiffness of this nonlinear system for *Model V* can be obtained (Worden and Tomlinson 2001).

Note that as it is shown by previous researchers (Taniguchi *et al.* 2008, Tsai 1995), isolation leads to

reductions in story drifts relative to the conventional buildings. As a result, the majority of the deformations in a base isolated structure are concentrated at the base isolation level. Therefore, to investigate the effects of the base isolator nonlinearities on the overall response of the system, the primary structure can be assumed as a generalized mass-spring-dashpot system with the total mass of the primary structure plus the mass of the isolator (i.e., $m_{bp}=m_{primary\ struc.}+m_b$). In the following derivations, the bp index denotes the properties of this generalized SDOF system.

The value of k_{eq} can be determined from this method by assuming that the system is stationary and is subjected to a phase-shifted sinusoidal excitation of $x_g(t)=X_g(t)\cdot\sin(\omega t-\phi)$. Now the trial harmonic balance solution $x_{bp}(t)=\mu D_y\cdot\sin(\omega t)$ can be considered to be substituted in the nonlinear equation of $f_s=k_{eq}x_{bp}$. The function that describes the force ($f_s(x_{bp})$), can also be expanded in terms of Fourier series

$$f_s(\mu D_y \sin(\omega t)) = a_0 + \sum_{n=1}^{\infty} a_n \cos(n\omega t) + \sum_{n=1}^{\infty} b_n \sin(n\omega t) \quad (14)$$

It could be shown that for purely odd stiffness functions (i.e., $f_s(-x_{bp})=-f_s(x_{bp})$), which is the case here, the values of $a_0=a_1=0$. Thus, Eq. (14) becomes

$$f_s(\mu D_y \sin(\omega t)) \equiv b_1 \sin(\omega t) = k_{eq} \mu D_y \sin(\omega t) \quad (15)$$

which yields

$$k_{eq} = \frac{1}{\pi \mu D_y} \int_0^{2\pi} f_s(\mu D_y \sin(\omega t)) \sin(\theta) \cdot d\theta \quad (16)$$

so the Frequency Response Function (FRF) takes the form

$$\Lambda(\omega) = \frac{1}{k_{eq} - m_{bp} \omega^2 + i c_b \omega} \quad (17)$$

The physical content of Eq. (16) can be explained as follows. This equation represents the average value of the restoring force over one cycle of excitation, divided by the value of the displacement. This gives a mean value of the stiffness experienced by the system over a cycle. For systems that can be approximated with piecewise linear model, which is of interest in this study, f_s could be written as follows

$$f_s(x_{bp}) = \begin{cases} k_y x_{bp} + (k_e - k_y) D_y & \text{when } x_{bp} \geq D_y \\ k_e x_{bp} & \text{when } |x_{bp}| < D_y \\ k_y x_{bp} - (k_e - k_y) D_y & \text{when } x_{bp} < -D_y \end{cases} \quad (18)$$

After replacing Eq. (18) into Eq. (16), the integrand changes for different values of x_{bp} with respects to D_y . This corresponds to a point in the cycle where $\theta_e = \sin^{-1}(\mu^{-1})$

$$k_{eq} = k_e + \frac{(k_y - k_e)}{\pi} \int_{\theta_e}^{\pi - \theta_e} \sin \theta \cdot \left(\sin \theta - \frac{x_e}{\mu D_y} \right) \cdot d\theta + \frac{(k_y - k_e)}{\pi} \int_{\pi + \theta_e}^{2\pi - \theta_e} \sin \theta \cdot \left(\sin \theta + \frac{x_e}{\mu D_y} \right) \cdot d\theta \quad (19)$$

It can be shown that the equivalent stiffness has the form

$$k_{eq} = k_e \left[1 + \frac{(\alpha - 1)}{\pi} \left\{ \pi - 2 \sin^{-1}(\mu^{-1}) - \frac{2}{\mu^2} \sqrt{\mu^2 - 1} \right\} \right] \quad (20)$$

As a check, substituting $k_e=k_y$ or $\alpha=1$ and also $\mu=1$ yields $k_{eq}=k_e$ as expected.

2.3 Numerical simulation

To investigate the effects of the nonlinearity of the BITMD system, a 5-storey benchmark base isolated structure is used. For the purpose of the design, a 7DOF system (i.e., one DOF for the base isolator, five DOFs for the primary structure, and one DOF for the TMD) is considered and using the five different models which were defined in the previous section, TMDs are designed. For each of these models, nonlinear response history analyses are carried out in OpenSees (McKenna *et al.* 2000). The 5-storey base isolated structure with properties similar to one considered in both Kelly *et al.* (2000) and Zhang and Phillips (2015) is used here where the dynamic parameters for representing a full-scale structure are chosen and shown in Table 1. The total mass of the primary structure $m_p=265.36$ tons so m_{bp} is equal to 326.57 tons. The natural period of vibration of the primary structure (fixed-based structure) is 0.54 s and the damping ratio in the first mode is 2%. schematic

To idealize the hysteretic behaviour of the isolator for the nonlinear system by the piecewise linear model in Fig. 2(b), all of the characteristic parameters (i.e., yield strength, Q_y , pre- and post-yield stiffness, k_e and k_y) have to be defined. The pre-yield stiffness, k_e , of the nonlinear system can be assumed to be equal to the stiffness of the linear base isolation system of *Model I* and the value of 0.10 is chosen for the post- to pre-yield stiffness ratio (α), which can be considered as an average of values suggested in the literature (Alhan and Sürmeli 2011). The yield strength, Q_y , may be selected within a suitable range depending on the value of the vertical force $W_{bp}=m_{bp}g$ due to the weight of the structure, including also the weight of the isolator. Based on values proposed in the literature, $Q_y = 0.05 \sim 0.20 W_{bp}$ can be used (Alhan and Sürmeli 2011). In this study, the value of 0.10 is chosen. Table 2 summarizes the values of the k_{eq} and corresponding k_t value for different models.

Table 1 Parameters of the 5-Story base-isolated structure model (Zhang and Phillips 2015)

Floor	Floor mass (kg)	Story stiffness (kN/m)	Damping coefficient (kN.s/m)
Base	$m_b = 61,200$	$k_e = 2,130$	$c_b = 69.94$
1	$m_1 = 53,073$	$k_1 = 101,196$	$c_1 = 348.14$
2	$m_2 = 53,073$	$k_2 = 87,279$	$c_2 = 301.38$
3	$m_3 = 53,073$	$k_3 = 85,863$	$c_3 = 296.18$
4	$m_4 = 53,073$	$k_4 = 74,862$	$c_4 = 259.81$
5	$m_5 = 53,073$	$k_5 = 57,177$	$c_5 = 197.45$

With the introduction of the base isolation system, the fundamental elastic period of vibration of the primary structure increases to 2.50 s. As the control case and in order to provide the reader with the response of the 5-story base isolated structure when the base isolators behave linearly, Fig. 3 shows the base isolation displacement of these systems with (*Model I*) and without TMDs. This figure confirms the findings of previous studies, and it can be seen that the incorporation of the TMD reduces the response at the resonance frequency considerably. As expected, even in the absence of the TMD, when the base isolation system behaves nonlinearly, the maximum displacement decreases significantly.

In Fig. 4, the nonlinear base isolated structure is equipped with a TMD (*Model III*) and the response time history is compared to that of the uncontrolled nonlinear base isolated system. As it can be seen in this figure, not only the introduction of the TMD does not reduce the maximum base isolation displacement, but also increases it by approximately 6%. However, after the first peak, the incorporated TMD affects the system and a constant reduction in the displacement can be observed. This can be explained by the fact that TMDs require a motion for activation so they are not very efficient in reducing the first peak but after getting activated they can reduce the response consistently.

As it was shown in Fig. 4, the application of the maximum base isolation displacement may not be sufficient to describe the effectiveness of the TMDs. Similar to many other nonlinear systems, other performance criteria can be used to provide a better insight into the effects of this control technique. To assess the performance of the proposed control strategy, a set of six performance criteria as shown in Table 3 are proposed. In this table, the response parameters of the nonlinear BITMD without the TMD appear with the 0 subscript, and similarly, the corresponding response parameters of the controlled nonlinear BITMD (*Model III*) is denoted by *t*.

Table 2 Values of the k_{eq} and k_t for different models

	Model I	Model II	Model III	Model IV	Model V
	Linear	Bouc-Wen	Bouc-Wen	Bouc-Wen	Bouc-Wen
k_{eq} (kN/m)	2,130	2,130	213	692	817
k_t (kN/m)	1,859	1,859	186	604	713

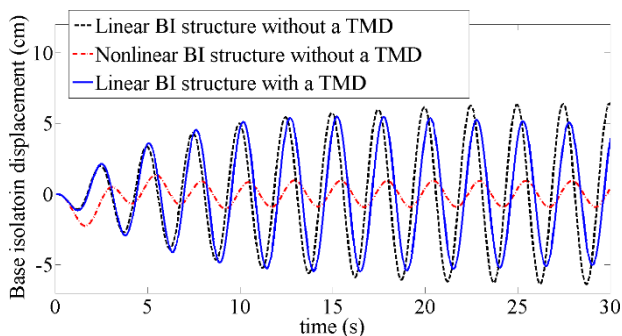


Fig. 3 Base isolation displacement of original systems

The summary of the calculated performance indices for the input ground acceleration of this section is shown in Table 4. Note when these indices indicate smaller than one values, it means that the control technique was successful in reducing the system response. For instance, J_5 can be used to monitor the higher modes effects in these two systems. Lower interstory drifts are expected for structures that have a dominant fundamental mode and therefore, it is desirable to observe J_5 indices that are less than one. The cumulative absorbed (elastic strain plus hysteretic) energy gives an indication of the accumulated damage induced in the inelastic structures and lower absorbed energies for any seismic input energy result in less damage to the structure.

Table 4 shows that the incorporation of the TMD in general reduces the RMS of the base isolation displacement and is more efficient in reducing the maximum floor acceleration than the maximum displacements. However, this strategy increases the maximum base shear and peak interstory drifts. From Table 4 it is apparent that *Model III* is the most effective design in reducing the absorbed energy of the system.

A closer look at the steady-state responses of the time-histories in Fig. 5 confirms that the assumption in *Model III* results in the highest reduction of the displacements.

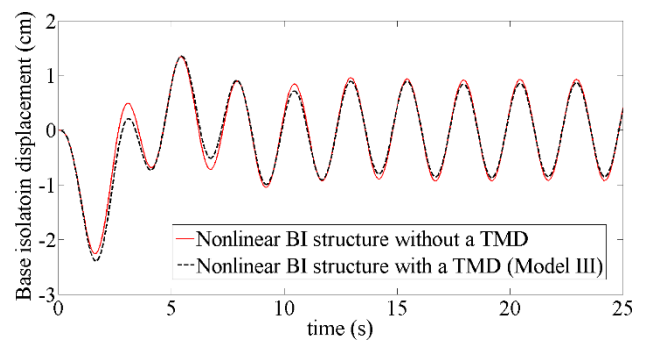


Fig. 4 Base isolation displacement of the nonlinear base isolated system with/without a TMD

Table 3 Performance indices

Peak Base Displacement:	RMS Base Displacement:	Peak Floor Acceleration:
$J_1 = \frac{\max\ x_t(t)\ }{\max\ x_o(t)\ }$	$J_2 = \frac{RMS\ (x_t(t))\ }{RMS\ (x_o(t))\ }$	$J_3 = \frac{\max\ \ddot{x}_t(t)\ }{\max\ \ddot{x}_o(t)\ }$
Peak Base Shear:	Peak Interstory Drift:	Max. Absorbed Energy:
$J_4 = \frac{\max\ V_t(t)\ }{\max\ V_o(t)\ }$	$J_5 = \frac{\max\ \Delta_t(t)\ }{\max\ \Delta_o(t)\ }$	$J_6 = \frac{\max\ AE_t(t)\ }{\max\ AE_o(t)\ }$

Table 4 Performance indices for the nonlinear base isolated structure with a TMD

	J1	J2	J3	J4	J5	J6
Model II	1.060	1.006	0.998	1.037	1.060	0.984
Model III	1.059	0.960	0.988	1.037	1.061	0.913
Model IV	1.063	0.990	0.996	1.039	1.066	0.957
Model V	1.063	0.994	0.997	1.040	1.066	0.964

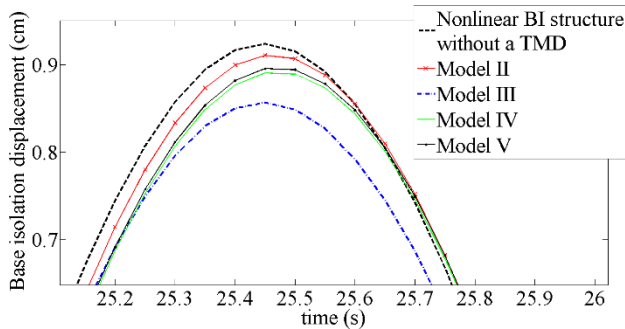


Fig. 5 Effectiveness of TMDs in nonlinear BITMD models with various assumptions about k_{eq}

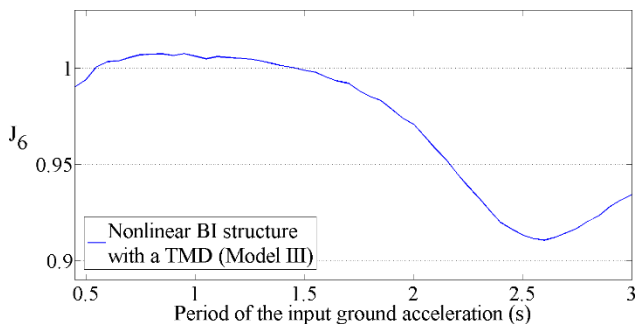


Fig. 6 Variation of J_6 for *Model III* with the frequency of the input ground acceleration

Therefore, it is recommended here that in the case of designing a TMD for a structure with a nonlinear base isolation system, the post-yield stiffness of the isolator should be selected as the equivalent stiffness of the base isolation element for designing the TMD.

From Table 4, it can also be concluded that J_6 should be used together with the displacement criteria to describe the effects of this control technique. The shown value is only for the sinusoidal input ground acceleration with a period of 2.50 seconds. To observe the variation of this performance index for other input ground accelerations, the period of the ground acceleration is changed in a range of 0.45 to 3.0 seconds and Fig. 6 is plotted. From Fig. 6, it can be seen that the incorporation of the TMD in *Model III* is most effective when the period of the input ground acceleration coincides with the resonant elastic period of the original system (i.e., around 2.50 s).

3. Parametric study

In the previous section, the analytical study showed that the introduction of the TMDs to base isolated systems with nonlinear base isolators subjected to harmonic ground excitation reduces the absorbed energy of the system, RMS of the base isolation displacement and maximum floor acceleration. It was also found that the assumption made for *Model III* leads to the best results and from this point forward, only this model will be used. In this section, the response reduction effects of TMDs on nonlinear BITMD systems will be examined for seismic ground motions. The performance of a BITMD system could be influenced by

Table 5 List of the earthquake ground motions considered in Section 3.1

Event	NGA #	Record Component	Mag.	R_{jb} (km)	PGA (g)	Type
Kern County (1952)	12	PEL090	7.36	114.62	0.042	Short period random phase type
Kern County (1952)	15	TAF111	7.36	38.42	0.178	Short period random phase type
Kobe (1995)	1106	KJM000	6.90	0.94	0.834	Mid-long pulse type
Kobe (1995)	1107	KAK000	6.90	22.50	0.195	Mid-long pulse type
Landers (1992)	879	LCN260	7.28	2.19	0.654	Long period fling step type
Landers (1992)	838	BRS000	7.28	34.86	0.108	Long period fling step type

several parameters such as the mass, frequency and damping ratios of the TMD, fundamental period of the structure, dynamic properties of the isolation system and properties of the input ground motion. To investigate this, dynamics models in OpenSees are selected with different levels of complexity and are studied in the time domain.

3.1 Input earthquake ground motion

A set of six different historical ground motions were selected from the PEER-NGA database (Pacific Earthquake Engineering Research Center 2015), and time history analyses were conducted with selected unscaled earthquake records. The details of each of the components of these ground motions are reported in Table 5. In this table, the corresponding record number (NGA #), moment magnitude (*Mag.*) and the closest horizontal distance to rupture plane (R_{jb}) of each component is shown. As it can be seen in this table, each pair of ground motion records represent a different kind of earthquakes.

Kern County (TAF111 and PEL090 in 1952), Kobe (KJM000 and KAK000, in 1995) and Landers (LCN260 and BRS000, in 1992) can be, respectively, classified into short period random phase type, mid-long pulse type and long period fling step type (Xiang and Nishitani 2014). Performance indices of Table 3 are calculated for each of these earthquakes, and the results are shown in Fig. 7.

Based on the results in Fig. 7, the incorporation of TMDs in base isolated structures with nonlinear base isolation systems is most effective when the system is subjected to a short period random phase type ground motion. Except for the case of LCN260, the maximum absorbed energy can be reduced by up to 33%. It can also be concluded that the control strategy is ineffective in reducing the maximum acceleration of the system and the maximum base displacement is more sensitive to the input ground motion than the maximum base acceleration. This applies to all six ground motions.

A closer look at Tables 5 and Fig. 7 also shows that in terms of reducing the absorbed energy, these systems are

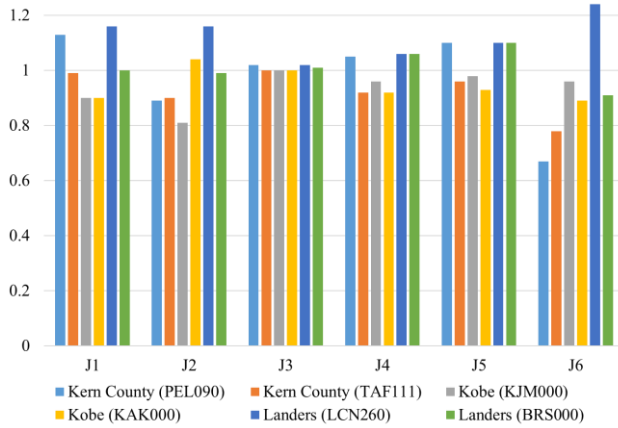


Fig. 7 Performance indices for the nonlinear BITMD under earthquake ground motions

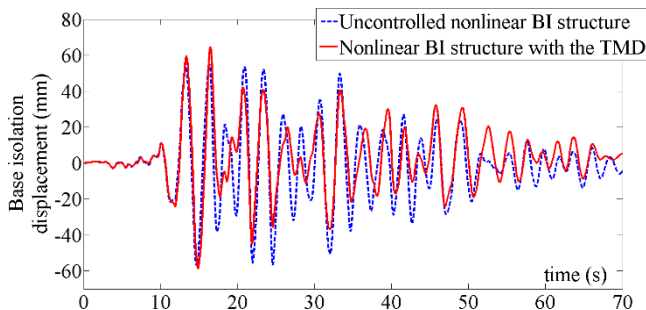


Fig. 8 Comparison between the base displacements nonlinear base isolated models with/without the TMD (Kern County - PEL090 ground motion)

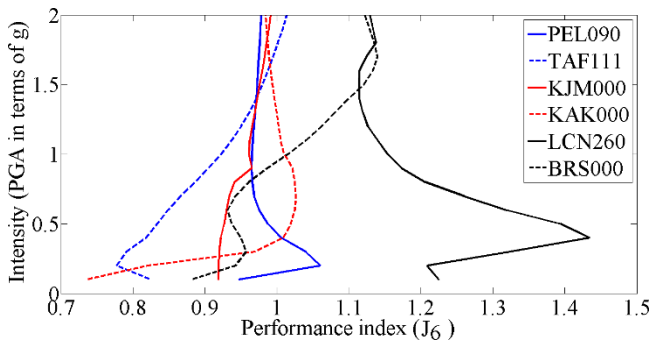


Fig. 9 Effects of earthquake intensity on the response of the system

more effective for cases in which the source of the earthquakes are further away from the structures. In Fig. 8, time histories of the base displacements (Kern County - PEL090 ground motion) are compared to better illustrate the effects of the introduction of TMDs in nonlinear base isolated structure. As it can be seen in this figure, although the maximum displacement is increased by 13 percent, the other peaks that follow the maximum displacement (between 18th and 35th seconds) have been reduced considerably. This is in agreement with the observations in Section 2.

It should be emphasized that the results highly depend on the characteristic of the input ground motion. Moreover,

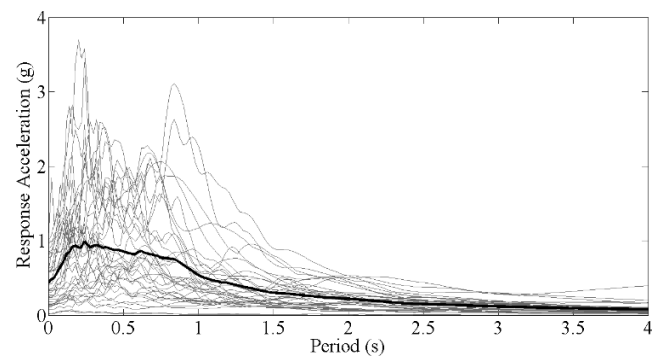
since the systems behave nonlinearly, the amplitude of the ground motion plays a significant role in the response of the system. To investigate the effects of the intensity of the input earthquake ground motions on the response, in Fig. 9, the scaling factor of the earthquakes are changed incrementally from zero to two.

An inspection of the results shows that except long period fling step type ground motions the incorporation of TMDs reduces the absorbed energy of the systems for common ground motions with intensities less than g . Mid-long pulse type ground motions are also less sensitive to the changes of the earthquake intensity.

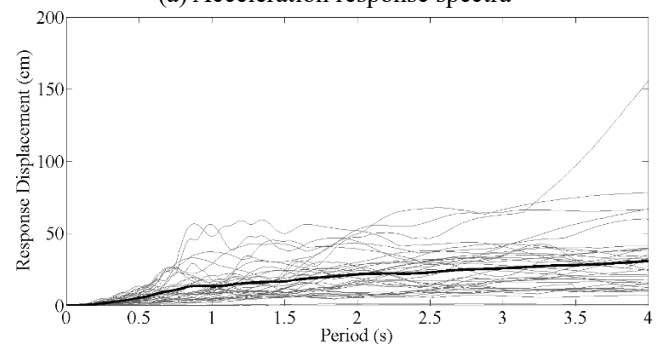
3.2 Yield strength and post-to pre-yield stiffness ratio of the base isolators

As it is shown in the previous section, the response of the nonlinear BITMD systems highly depends on the choice of the ground motion record and its characteristics. Therefore, the number of considered ground motion records are increased in this section and the following sections to obtain more reliable conclusions. A set of 18 different historical ground motions are selected from the PEER-NGA database, and time history analyses are performed. Both of the horizontal components of the records are applied, and the resulting performance criteria are recorded.

Details of each of the components of these ground motions are reported in Table 6. It can be seen that both near- and far-field ground motions are included in this list (Taniguchi *et al.* 2008, Mirza Hessabi and Mercan 2016). The elastic response spectra of the unscaled records are shown in Fig. 10 where, the average spectrum for these records is shown with a solid black line. As it can be seen in



(a) Acceleration response spectra



(b) Displacement response spectra

Fig. 10 Response spectra for the 36 ground motion records

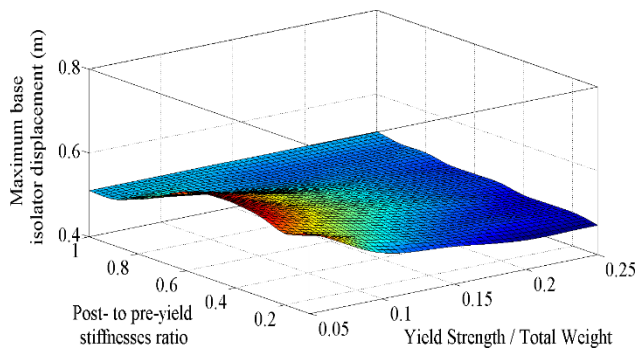


Fig. 11 Effects of the values of Q_y and α on the system response

this figure, the considered ground motion records cover a broad range of earthquakes with different properties. To examine the sensitivity of the response of a system to the nonlinearities of the base isolator, the yield strength, and post- to pre-yield stiffness ratio of these elements are changed. The former parameter is normalized by the weight of the structure.

Fig. 11 illustrates the variation of the response for these two parameters. The values used in this figure are the average of the RMS of the base displacements for the set of 36 earthquake ground motions which are listed in Table 6.

The contours of the relations between these parameters are shown in Fig. 12. From Figs. 11-12, it can be concluded that the combination of Q_y and α can result in different system responses and appropriate selection of a combination of these variables should be made during the design procedure of the base isolation systems. As a general observation, as already found by previous researchers in other systems, the effectiveness of the TMD deteriorates with the increase of the size of the hysteresis and higher displacements are expected for lower Q_y over weight ratios.

3.3 Mass ratio of the TMD and damping ratio of the primary structure

The design of tuned mass damper involves the selection of mass ratio, frequency tuning and damping parameter. It is usually desirable to use a small mass ratio to introduce a minimum undesirable extra weight in the structure. However, it is important to study the effects of this parameter on the overall performance of this hybrid control strategy. The same set of 36 earthquake ground motions are used in this section. When looking at the averaged RMS of the base displacements in Fig. 13, it can be concluded that the introduction of TMDs to the nonlinear systems is more effective for primary systems with lower inherent damping ratios. In addition, the increase of the TMD mass ratio has the effect of reducing the system demand. It is clear that TMD mass ratio and structure damping ratio are less effective when the RMS of the response is considered.

3.4 Natural period of the superstructure and the location of the TMD

To design a TMD for the base isolated structure, most of

Table 6 List of the earthquake ground motions considered in Sections 3.2 - 3.5

	Event	NGA #	Record Component	Mag.	R _{jb} (km)	PGA (g)
1	Loma Prieta	799	SFO090	6.93	58.52	0.329
2	Loma Prieta	799	SFO000	6.93	58.52	0.236
3	Loma Prieta	738	NAS180	6.93	70.90	0.268
4	Loma Prieta	738	NAS270	6.93	70.90	0.209
5	Imperial Valley	169	H-DLT352	6.53	22.00	0.351
6	Imperial Valley	169	H-DLT262	6.53	22.00	0.238
7	Kobe	1107	KAK090	6.90	22.50	0.345
8	Kobe	1107	KAK000	6.90	22.50	0.251
9	Chi-Chi, Taiwan	1487	TCU047-N	7.62	35.00	0.413
10	Chi-Chi, Taiwan	1487	TCU047-E	7.62	35.00	0.301
11	Kern County	15	TAF111	7.36	38.42	0.178
12	Kern County	15	TAF021	7.36	38.42	0.156
13	Landers	838	BRS000	7.28	35.90	0.132
14	Landers	838	BRS090	7.28	34.90	0.135
15	Chi-Chi, Taiwan - 06	3317	CHY101-N	6.30	34.50	0.146
16	Chi-Chi, Taiwan - 06	3317	CHY101-E	6.30	34.50	0.127
17	N. Palm Springs	532	CLJ000	6.06	78.10	0.021
18	N. Palm Springs	532	CLJ090	6.06	78.10	0.019
19	Northridge	1044	NWH090	6.69	5.90	0.583
20	Northridge	1044	NWH360	6.69	5.90	0.590
21	Loma Prieta	779	LGP000	6.93	3.88	0.966
22	Loma Prieta	779	LGP090	6.93	3.88	0.587
23	Imperial Valley	183	H-E08140	6.53	3.90	0.602
24	Imperial Valley	183	H-E08230	6.53	3.90	0.454
25	Imperial Valley - 06	160	H-BCR140	6.53	2.70	0.588
26	Imperial Valley - 06	160	H-BCR230	6.53	2.70	0.775
27	Kobe	1106	KJM000	6.90	0.94	0.821
28	Kobe	1106	KJM090	6.90	0.94	0.599
29	Chi-Chi, Taiwan	1549	TCU129-E	7.62	1.84	1.010
30	Chi-Chi, Taiwan	1549	TCU129-N	7.62	1.84	0.634
31	Chi-Chi, Taiwan	1231	CHY080-E	7.62	2.70	0.968
32	Chi-Chi, Taiwan	1231	CHY080-N	7.62	2.70	0.902
33	Tabas, Iran	143	TAB-TR	7.35	2.00	0.852
34	Tabas, Iran	143	TAB-LN	7.35	2.00	0.836
35	Duzce, Turkey	1611	1058-E	7.14	0.2	0.111
36	Duzce, Turkey	1611	1058-N	7.14	0.2	0.073

the studies currently recommend replacing the entire primary structure by an equivalent DOF for which the lumped mass is equal to the total mass of the primary structure. In this section, nonlinear response history analyses are carried out to evaluate the accuracy of this simplification and study the effects of the natural period of the superstructure on the performance of BITMDs. Three models are defined in this section: in the first model the TMD is mounted on the top of the primary structure (*System I*). In the second model, the traditional TMD is placed on top of the base isolator (*System II*). In this model, the viscous damper is connected between the base isolator and the TMD. In the third model, the proposed model of Xiang and Nishitani (2014) is used in which the TMD is directly connected to the ground with a dashpot (*System III*). These systems are shown in Fig. 14. The selected structural properties in this section are similar to ones considered in (Yang *et al.* 1990) where the mass of each floor of the primary structure is assumed to be 300 tons, and the isolator mass is equal to 400 tons. The stand-alone base-isolated structure considered for the analysis has a damping ratio of 0.05 and a period of 2.0 s. The rest of the design parameters are defined as explained in Section 2. In different analyses, a family of shear story buildings with a different number of stories of the primary structure are subjected to the set of 36 ground motion records and their responses have been averaged. Typical stiffness of each story, k_i , can be calculated as follows

$$k_i = \left(\frac{2\pi}{T_p} \right)^2 \left(\frac{\sum_{j=1}^N u_j^2}{\sum_{j=1}^N u_j} \right) \cdot m_i \quad (21)$$

where, u_j is the deflection due to the associated applied static force at the j th degree of freedom. The typical damping of each story is also assumed to be proportional to k_i . The performance of these systems are listed in Table 7.

An inspection of the reported results in Table 7 reveals that the incorporation of the TMDs in nonlinear base isolated structures is most effective when the device is located at the top level of the primary structure (i.e., *System I*). In addition, the effectiveness of this control strategy increases for higher buildings with longer periods of vibration.

5. Conclusions

This paper studies the effects of the base isolation nonlinearities on the seismic performance of base isolated structures equipped with tuned mass dampers. The obtained conclusions can be summarized as follows.

- To consider the effects of the nonlinearities of base isolation systems, a Bouc-Wen model is used and using OpenSees, several numerical time-history simulations are performed.
- In general, the effectiveness of the incorporation of TMDs in base isolated structures with nonlinear base isolation systems is not as significant as for linear base isolation systems. The performance of these devices in nonlinear systems highly depends on the system parameters and input ground motion characteristics. However, as it is shown in this paper, there are still many scenarios in which TMDs can still improve the performance of the base isolated structures successfully.

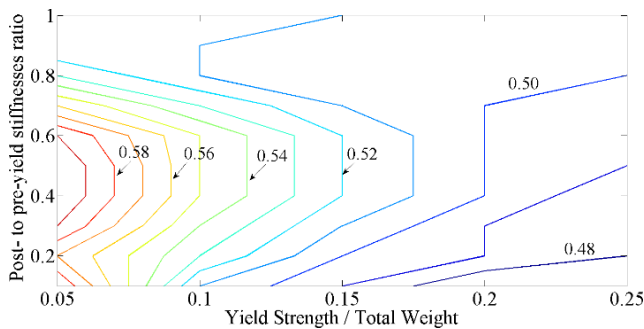


Fig. 12 Relationship between the effects of Q_y and α values on the system response

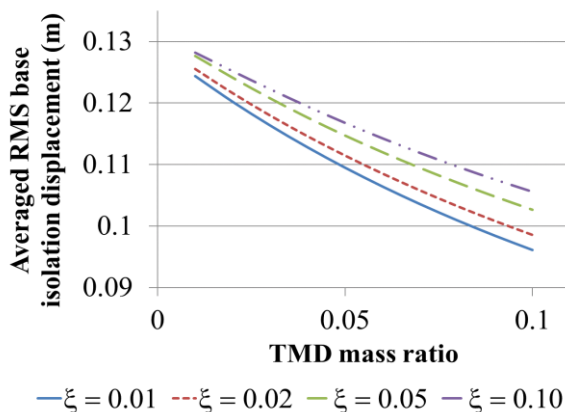


Fig. 13 The effects of TMD mass ratio and damping of the primary structure on the RMS of the system response

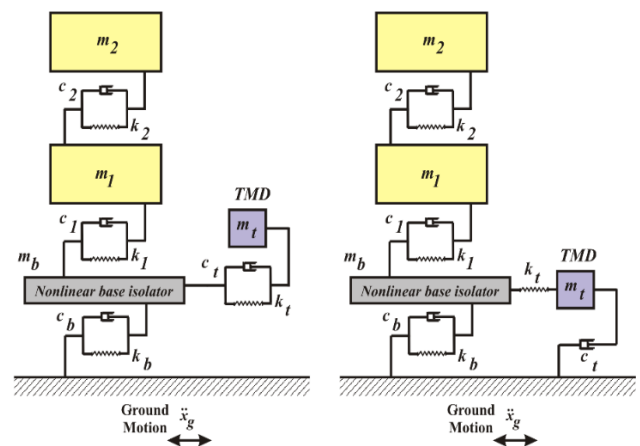


Fig. 14 Analytic models of three BITMD systems with 2DOF superstructures: a traditional TMD on the base isolation system (left), and a nontraditional TMD of (Xiang and Nishitani 2014) on the base isolation system (right)

Table 7 Performance indices for different systems of Fig. 14

		J1	J2	J3	J4	J5	J6
5 story super- structure	System I	0.89	0.89	1.00	0.95	1.00	0.97
	System II	0.91	0.91	1.00	0.96	0.86	0.98
	System III	0.92	0.92	1.03	0.96	1.00	1.02
10 story super- structure	System I	0.86	0.86	1.02	0.93	0.96	0.96
	System II	0.93	0.93	1.01	0.96	0.87	0.99
	System III	0.94	0.94	1.02	0.97	1.01	1.01
15 story super- structure	System I	0.84	0.84	1.03	0.93	0.94	0.95
	System II	0.98	0.98	1.00	0.98	0.89	1.01
	System III	0.98	0.98	1.02	0.98	1.02	1.01
20 story super- structure	System I	0.79	0.79	1.03	0.87	0.90	0.94
	System II	1.03	1.03	1.00	1.01	0.93	1.03
	System III	1.01	1.01	1.00	0.99	1.02	0.99

- In the case of the application of a TMD in a nonlinear system, it is always important to choose the right equivalent stiffness for the nonlinear elements before designing the TMD. In this study, several models were considered and it was found that the post-yield stiffness of the isolator should be selected as the equivalent stiffness of the base isolation element for designing the TMD.

- Unlike in BITMD systems with linear base isolation systems, the maximum base isolation displacement may not be sufficient to give a good indication of the TMD effectiveness. After the activation of the TMD, significant reductions in the displacements may occur and consequently with the introduction of a TMD the absorbed energy may be reduced significantly. Since the absorbed energy of the system gives an indication of the accumulated damage induced in the inelastic structures, it is proposed here to use this parameter as a performance criterion, in conjunction with the peak and RMS of the base isolation displacements. It was also observed that the introduction of the TMD, does not affect the maximum acceleration of the system significantly.

- Although the response reduction effect of the TMD system degraded for long period fling step type ground motion, the TMD was reasonably effective in the BITMD with the nonlinear base isolation system subjected to short period random phase type ground motions. This can be due to the fact that the long-period ground motion contains fewer resonant components.

- Through several numerical simulations, it has been shown that the combination of yield strength (Q_y) and post- to pre-yield stiffness ratio (α) of the base isolator during particular earthquakes can result in different responses. In general, the effectiveness of the TMDs reduces when the area under the hysteresis of the nonlinear base isolators increases. Appropriate selection of a combination of these variables should be made during the design procedure of the base isolation

systems.

- The mass ratio of the TMD plays a relevant role in the BITMD performance setting. The highest effectiveness is achieved for higher mass ratios. However, the increase in the inherent damping of the primary structure leads to a reduction of the effectiveness of these devices.

- The TMD system is effective in the response reduction when the TMD is located at the top of the superstructure. However, the efficiency of the entire structural control system may vary for different input earthquake ground motions as the frequency content and intensity of the earthquake can force the system to resonate. A set of 18 different scaled historical ground motions were selected from the PEER-NGA database and time history analyses were performed. It was found that the effectiveness of the TMD for nonlinear BITMD systems increases when the superstructure is higher and has a longer fundamental period.

It should be noted that the numerical investigations in Section 3.1 only consider a limited number of earthquake ground motions and classify the records into short period random phase, mid-long pulse and long period fling step types. However, to understand the effects of the input earthquake parameters on the performance of these systems better, further studies with a larger suit of records required. Similar studies to Mirza Hessabi (2017), where a set of 99 typical ground motion records were used to examine records with large peak displacement, velocity, and acceleration, or large incremental velocity, and displacement can be used to investigate these effects more comprehensively. In particular, the effects of long duration intense velocity pulses in the horizontal direction, which are expected for near fault earthquakes can be studied in future. In addition, further studies must be conducted to assess the performance of TMDs and multiple tuned mass dampers (MTMDs) in real 3-dimensional building models with nonlinear base isolation systems such as triple friction pendulum bearings.

References

- Alhan, C. and Gavin, H. (2004), "A parametric study of linear and non-linear passively damped seismic isolation systems for buildings", *Eng. Struct.*, **26**(4), 485-497.
- Alhan, C. and Sürmeli, M. (2011), "Shear building representations of seismically isolated buildings", *Bull. Earthq. Eng.*, **9**(5), 1643-1671.
- Chung, L.L., Wu, L.Y., Huang, H.H., Chang, C.H. and Lien, K.H. (2009), "Optimal design theories of tuned mass dampers with nonlinear viscous damping", *Earthq. Eng. Eng. Vib.*, **8**(4), 547-560.
- De Iuliis, M., Petti, L. and Palazzo, B. (2008), "Effect of tuned mass damper on displacement demand of base-isolated structures", *Eng. Struct.*, **30**(12), 3478-3488.
- Den Hartog, J.P. (1985), *Mechanical Vibrations*, 4th edition, McGraw-Hill, New York, USA.
- Esteki, K., Bagchi, A. and Sedaghati, R. (2015), "Semi-active control of seismic response of a building using MR fluid-based tuned mass damper", *Smart Struct. Syst.*, **16**(5), 807-833.
- Ikhoulane, F., Mañosa, V. and Rodellar, J. (2007), "Dynamic

- properties of the hysteretic Bouc-Wen model”, *Syst. Control Lett.*, **56**(3), 197-205.
- Jennings, P.C. (1968), “Equivalent viscous damping for yielding structures”, *J. Eng. Mech. Div.*, **94**(1), 103-116.
- Kelly, J.M. (1999), “The role of damping in seismic isolation”, *Earthq. Eng. Struct. Dyn.*, **28**(1), 3-20.
- Kelly, J.M., Leitmann, G. and Soldatos, A.G. (1987), “Robust control of base-isolated structures under earthquake excitation”, *J. Optimiz. Theory Appl.*, **53**(2), 159-180.
- Mahmoud, S., Austrell, P.E. and Jankowski, R. (2012), “Simulation of the response of base-isolated buildings under earthquake excitations considering soil flexibility”, *Earthq. Eng. Eng. Vib.*, **11**(3), 359-374.
- Matta, E. (2015), “Seismic effectiveness of tuned mass dampers in a life-cycle cost perspective”, *Earthq. Struct.*, **9**(1), 73-91.
- Mazza, F. and Vulcano, A. (2009), “Nonlinear response of RC framed buildings with isolation and supplemental damping at the base subjected to near-fault earthquakes”, *J. Earthq. Eng.*, **13**(5), 690-715.
- McKenna, F., Fenves, G.L., Scott, M.H. and Jeremic, B. (2000), *Open System for Earthquake Engineering Simulation (OpenSees)*, Pacific Earthquake Engineering Research Center, University of California, Berkeley, CA.
- Mirza Hessabi, R. (2017), *Application of real-time hybrid simulation method in experimental identification of gyromass dampers*, Ph.D. Dissertation, Civil Engineering Department, University of Toronto, Canada.
- Mirza Hessabi, R. and Mercan, O. (2016), “Investigations of the application of gyro-mass dampers with various types of supplemental dampers for vibration control of building structures”, *Eng. Struct.*, **126**, 174-186.
- Mirza Hessabi, R., Mercan, O. and Ozturk, B. (2014), “The effects of tuned mass dampers on seismic performance of structures with nonlinear base isolators: a parametric study”, *Proceedings of the 6th World Conference on Structural Control and Health Monitoring (6WCSCM)*, Barcelona, Spain, July.
- Pacific Earthquake Engineering Research Center, Regents of the University of California, Berkeley (2015), Next Generation Attenuation Relationships - Strongmotion Database, Berkeley, USA. Retrieved from <http://ngawest2.berkeley.edu/>.
- Palazzo, B. and Petti, L. (1999), “Combined control strategy: base isolation and tuned mass damping”, *ISET J. Earthq. Technol.*, **36**(2-4), 121-137.
- Palazzo, B., Petti, L. and de Ligio, M. (1997), “Response of base isolated systems equipped with tuned mass dampers to random excitations”, *J. Struct. Control*, **4**(1), 9-22.
- Petti, L., Giannattasio, G., De Iuliis, M. and Palazzo, B. (2010), “Small scale experimental testing to verify the effectiveness of the base isolation and tuned mass dampers combined control strategy”, *Smart Struct. Syst.*, **6**(1), 57-72.
- Politopoulos, I. (2008), “A review of adverse effects of damping in seismic isolation”, *Earthq. Eng. Struct. Dyn.*, **37**(3), 447-465.
- Ribakov, Y. (2010), “Reduction of structural response to near fault earthquakes by seismic isolation columns and variable friction dampers”, *Earthq. Eng. Eng. Vib.*, **9**(1), 113-122.
- Sinha, S.C. and Li, G. (1994), “Optimal design of base-isolated structure with dynamic absorbers”, *J. Eng. Mech.*, **120**(2), 221-231.
- Taniguchi, T., Der Kiureghian, A. and Melkumyan, M. (2008), “Effect of tuned mass damper on displacement demand of base-isolated structures”, *Eng. Struct.*, **30**(12), 3478-3488.
- Tsai, H. (1995), “The effect of tuned-mass dampers on the seismic response of base-isolated structures”, *Int. J. Solid. Struct.*, **32**(8-9), 1195-1210.
- Tsai, H-C. and Lin, G-C. (1993), “Optimum tuned-mass dampers for minimizing steady-state response of support-excited and damped systems”, *Earthq. Eng. Struct. Dyn.*, **22**(11), 957-973.
- Wen, Y.K. (1976), “Method for random vibration of hysteretic systems”, *J. Eng. Mech.*, **102**(2), 249-263.
- Worden, K. and Tomlinson, G.R. (2001), *Nonlinearity in Structural Dynamics: Detection, Identification and Modeling*, Institute of Physics Publishing, Bristol, Philadelphia, USA.
- Xiang, P. and Nishitani, A. (2014), “Optimum design for more effective tuned mass damper system and its application to base-isolated buildings”, *Struct. Control Health Monit.*, **21**(1), 98-114.
- Yang, J.N., Danielians, A. and Liu, S.C. (1990), “Aseismic hybrid control system for building structures under strong earthquake”, *J. Intel. Mater. Syst. Struct.*, **1**(4), 432-446.
- Zhang, R. and Phillips, B.M. (2015), “Performance and protection of base-isolated structures under blast loading”, *J. Eng. Mech.*, 04015063.

CC